Zero order synthetic hologram with a sinusoidal phase carrier for generation of multiple beams

V. Arrizón[1], U. Ruiz[1], G. Mendez[1], and A. Apolinar-Iribe[2]

[1]Instituto Nacional de Astrofísica, Optica y Electrónica,
Apartado Postal 51 y 216, Puebla PUE 72000, México.
[2]Departamento de Física, Universidad de Sonora (UNISON),
Apdo. Postal 1626, C. P. 83000, Hermosillo, Sonora, México.
arrizon@inaoep.mx

Abstract: We discuss a phase synthetic hologram, for encoding arbitrary complex fields, whose design is based on a sinusoidal phase grating with a spatially modulated phase depth. An important feature of the hologram is that it encodes the complex field at the zero diffraction order of the carrier grating. The smoothness of this sinusoidal carrier grating facilitates the implementation of the hologram with a pixelated spatial light modulator. We take advantage of the hologram reconstruction at the zero-diffraction order for the simultaneous generation of a collection of complex beams.

OCIS codes: (090.1760) Computer holography; (230.6120) Spatial light modulators; (070.0070) Fourier optics and optical signal processing; (190.4223) Nonlinear wave mixing

References and links

1. J. Arlt, T. Hitomi, and K. Dholakia, "Atom guiding along Laguerre-Gaussian and Bessel light beams," Appl. Phys. B **71**, 549–554 (2000).
2. T. Kuga, Y. Torii, N. Shiokawa, T. Hirano, Y. Shimizu, and H. Sasada, "Novel Optical Trap of Atoms with a Doughnut Beam," Phys. Rev. Lett. **78**, 4713-4716 (1997).
3. A. Bezryadina, D. N. Neshev, A. S. Desyatnikov, J. Young, Z. Chen, and Y. S. Kivshar, "Observation of topological transformations of optical vortices in two-dimensional photonic lattices," Opt. Express **14**, 8318-8327, (2006).
4. D. Sánchez-de-la-Llave, V. Arrizón, and L. A. Gonzalez, "Isotropic edge enhancement filter implemented with a phase-only spatial light modulator," Proc. SPIE **4471**, 114-123 (2001).
5. S. Fürhapter, A. Jesacher, S. Bernet, and M. Ritsch-Marte, "Spiral phase contrast imaging in microscopy," Opt. Express **13**, 689-694 (2005).
6. R. W. Cohn and M. Liang, "Approximating fully complex spatial modulation with pseudorandom phase-only modulation," Appl. Opt. **33**, 4406–4415 (1994).
7. V. Kettunen, P. Vahimaa, J. Turunen, and E. Noponen, "Zeroth-order coding of complex amplitude in two dimensions," J. Opt. Soc. Am. A **14**, 808-815 (1997).
8. D. Mendlovic, G. Shabtay, U. Levi, Z. Zalevsky, and E. Marom, "Encoding technique for design of zero-order (on-axis) Fraunhofer computer-generated holograms," Appl. Opt. **36**, 8427-8434 (1997).
9. J. A. Davis, D. M. Cottrell, J. Campos, M. J. Yzuel, and I. Moreno, "Encoding amplitude information onto phase-only filters," Appl. Opt. **38**, 5004-5013 (1999).
10. M. A. A. Neil, T. Wilson, and R. Juškaitis, "A wavefront generator for complex pupil function synthesis and point spread function engineering," J. Microsc. **197**, 219-223 (2000).
11. V. Arrizón, "Optimum on-axis computer-generated hologram encoded into low-resolution phase-modulation devices," Opt. Lett. **28**, 2521-2523 (2003).
12. V. Arrizón, U. Ruiz, R. Carrada, and L. A. González, "Pixelated phase computer holograms for the accurate encoding of scalar complex fields," J. Opt. Soc. Am. A **24**, 3500-3507 (2007).
13. W. J. Dallas, "Computer-generated holograms" in *The Computer in Optical Research*, B. R. Frieden, ed., (Springer-Verlag, Berlin. 1980), pp. 4156-4165.
14. A. Apolinar-Iribe, N. Korneev, V. Vysloukh and C. M. Gómez-Sarabia, "Transverse modulational instability of periodic light patterns in photorefractive strontium barium niobate crystal," Opt. Lett. **27**, 2088-2090 (2002).
15. V. Arrizón, S. Chavez-Cerda, U. Ruiz, and R. Carrada, "Periodic and quasi-periodic non-diffracting wave fields generated by superposition of multiple Bessel beams," Opt. Express **15**, 16748-16753 (2007).

#105592 - $15.00 USD Received 19 Dec 2008; revised 29 Jan 2009; accepted 6 Feb 2009; published 10 Feb 2009

1. Introduction

Transformation of a laser beam into an arbitrary complex field is required in several optical applications, e. g. atom optical trapping and guiding [1, 2], photonic lattices [3], and optical processing [4,5]. This transformation can be performed, in a robust and versatile way, by means of synthetic phase holograms (SPHs) [6-12]. Recently we reported [12] two SPHs that encode a complex field in the first diffraction order of a sinusoidal carrier grating. These SPHs show a relatively smooth spatial variation of phase modulation, which facilitates its accurate implementation with an electrically addressable spatial light modulator (SLM). Here we discuss a SPH that also employs a sinusoidal carrier, for which the encoded complex field appears at the zero order of the hologram Fourier series. We show that this hologram is useful for the appropriate generation of a collection of different complex beams. When the SPH is implemented with a pixelated SLM, the available spatial frequency bandwidth for encoding the complex beams is relatively small. In order to make an efficient use of this limited SLM bandwidth, the beams are generated in such a way that they propagate on axes that are symmetrically arranged around the optical axis. In other words, the Fourier spectrum of the collection of beams appears centered at the axis of the spatial frequency domain.

2. The zero order synthetic phase hologram: Basic theory

It is assumed that the hologram is applied for encoding a scalar complex field

$$s(x, y) = a(x, y)\exp[i\phi(x, y)], \tag{1}$$

whose amplitude $a(x,y)$ and phase $\phi(x,y)$ take values in the real domains [0,1] and [-π,π] respectively. In order to specify a phase hologram encoding the complex field $s(x,y)$, we first obtain a phase hologram, $h_a(x,y)$, which only encodes the amplitude $a(x,y)$, and then we determine the SPH transmittance

$$h(x, y) = h_a(x, y)\exp[i\phi(x, y)], \tag{2}$$

for encoding the complex field $s(x,y)$. The transmittance of the SPH that we propose to encode the amplitude $a(x,y)$ has the form

$$h_a(x, y) = \exp\{if(a)\sin[2\pi(u_0 x + v_0 y)]\}. \tag{3}$$

This SPH is essentially an oblique sinusoidal phase grating, whose phase depth is spatially modulated by the factor $f[a(x,y)]$. In order to determine this phase modulation we employ the Jacoby-Anger identity to express the hologram transmittance by its Fourier series

$$h_a(x, y) = \sum_{q=-\infty}^{\infty} J_q[f(a)]\exp[i2\pi(qu_0 x + qv_0 y)], \tag{4}$$

where J_q represents a q-th integer order Bessel function of the first kind. The amplitude $a(x,y)$ can be encoded with the zero order term of this Fourier series by assuming that the identity

$$J_0[f(a(x, y))] = a(x, y), \tag{5}$$

holds for every point (x,y) where $a(x,y)$ is defined. The fulfillment of this relation, which is referred to as the encoding condition, is ensured by obtaining $f(a)$ from the numerical inversion of Eq. (5). According to Eq. (2), the zero order phase hologram that encodes the complex field $s(x,y)$ is given by

$$h(x, y) = \exp[i\phi(x, y)]\exp\{if(a)\sin[2\pi(u_0 x + v_0 y)]\}. \tag{6}$$

This SPH does not require a structured cell to encode each pixel of the complex field, thus it is classified as a point-oriented hologram [13]. In general, if a hologram is implemented with a pixelated SLM it is convenient to design it using a point-oriented approach. The SPH

#105592 - $15.00 USD Received 19 Dec 2008; revised 29 Jan 2009; accepted 6 Feb 2009; published 10 Feb 2009

transmittance in Eq. (6) represents the main result reported here. This SPH shows some similarities with the holograms reported in Ref. [12]. However, the phase modulation of the SPH transmittance in Eq. (6), given by $\phi(x,y)+f[a(x,y)]\sin[2\pi(u_0x+v_0y)]$, is essentially different to the phases of the SPHs discussed in Ref. (12) (see Eqs. (9), (12) and (16) of this cited paper). For the SPH specified in Eq. (6) the encoded complex field appears at the zero order of the SPH Fourier series. This feature represents an essential difference with the SPHs discussed in Ref. (12). A different zero order point-oriented SPH, based on a binary high frequency carrier, was reported in Ref. [11]. The performance of this last hologram, tested in numerical simulations, is quite satisfactory. However, its realization with an electrically addressable phase SLM tends to be deficient because of the difficulty that this device shows for implementing high frequency binary carriers. The effect of this difficulty is reduced by the use of a smooth carrier grating, in the zero order SPH specified in Eq. (6). To ensure the carrier smoothness in this hologram, the carrier frequencies (u_0,v_0) must be smaller than the spatial frequency bandwidth of the SLM employed to implement it. Obviously, this condition imposes a limit to the bandwidth of the fields that can be accurately encoded by this hologram.

A generalized form of the zero-order SPH defined in Eq. (6) can be, in principle, obtained by replacing the sinusoidal carrier function by other periodic functions. However, among the different choices, the SPH with sinusoidal carrier has the remarkable feature of a q-th order term in its Fourier series given by the factor $J_q[f(a)]\exp[i\phi(x,y)]$. As a consequence, the power content of the high order SPH terms shows a fast reduction with the order q. This is an advantage when the SPH is implemented with a pixelated SLM, because the high order terms that appear mounted to the zero order in a pixelated SPH, will introduce a relatively low noise amount. If the employed SLM has resolution δx and the carrier frequencies are $u_0=v_0=\Delta u/Q$, where $\Delta u=\delta x^{-1}$ is the SLM spatial frequency bandwidth, only the high order terms with indices multiple of Q appear mounted to the zero order term [12].

3. Application of SPHs for generation of multiple complex beams

The SPH specified in Eq. (6) will be numerically evaluated next as a tool for the simultaneous generation of multiple complex beams. This task is possible because the complex function to be encoded [Eq. (1)] can be the result of superposing a collection of complex functions, within a common support. We also assume that the beams corresponding to these complex functions propagate at different axes, which form small angles respect to the z-axis. Thus, such complex functions must be modulated by different linear phase carriers. As initial example we simulate the encoding of the complex field

$$s_1(x,y) = c\, J_1(2\pi\rho_0 r)\exp(i\theta)\,[\cos(2\pi\xi_0 y) + b\cos(2\pi\eta_0 x)]\,. \tag{7}$$

For simplicity, the complex amplitude of this field is specified using both rectangular (x,y) and polar (r,θ) coordinates. The complex field $s_1(x,y)$ is equivalent to 4 first-order non-diffracting Bessel beams of radial spatial frequency ρ_0, with different amplitudes and propagation axes. Two beams, generated by the factor $\cos(2\pi\xi_0 y)$, propagate on axes lying on the plane y-z, and the other two beams, generated by the factor $\cos(2\pi\eta_0 x)$, propagate on axes lying on the plane x-z. The constant c performs the normalization of the whole field $s_1(x,y)$. The field $s_1(x,y)$ is defined within a circular pupil of radius $R=128\delta x$, in such a way that the first positive root of the Bessel function $J_1[2\pi\rho_0 r]$ appears at the edge of this pupil. The spatial frequencies for the cosine carriers of beams are $\xi_0=\eta_0=\Delta u/24$.

We are presently studying the nonlinear interaction of the multiple beams that compose the complex field defined in Eq. (7) and variants of it [14]. The advances in this task are not reported here. In this context it is required that the beams propagating in the x-z plane show relatively low amplitudes. These amplitudes are controlled by the constant b, which in the next simulation is adopted as b=1/10. The holographic generation of multiple complex beams, including several low intensity beams, with low noise levels is challenging, due to the

#105592 - $15.00 USD Received 19 Dec 2008; revised 29 Jan 2009; accepted 6 Feb 2009; published 10 Feb 2009

multiple high order terms of most holograms. This difficulty is even greater for SPHs implemented with pixelated SLMs, for which the number and spatial density of high order noisy terms are substantially increased [12,15]. The modulus and phase of the complex field $s_1(x,y)$, together with the modulus of the Fourier spectrum of this field, are depicted in Fig. 1. We display the modulus instead of the intensity of the field Fourier spectrum in order to show appropriately the low amplitude features.

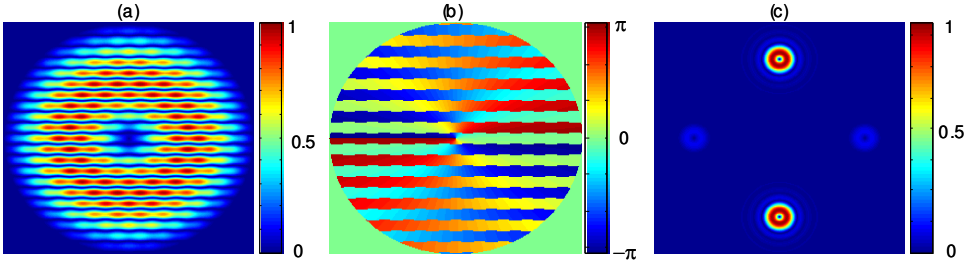

Fig. 1. (a). Modulus and (b). phase of the complex field $s_1(x,y)$, and (c). modulus of its Fourier spectrum.

Let us assume that the SPHs are implemented using a pixelated phase SLM. The SLM bandwidth is $\Delta u=1/\delta x$, where δx denotes the SLM spatial resolution. We assume, for the moment, that the spatial frequencies of the sinusoidal hologram carrier are $u_0=v_0=\Delta u/4$. The SPH of the field $s_1(x,y)$ is computed with Eq. (6). A partial view of the SPH Fourier spectrum modulus, depicted at Fig. 2(a), shows the central 4 spots, corresponding to the encoded beams in the complex field $s_1(x,y)$, and other spots that correspond to several high order terms of the SPH. A close view of the 4 central spots, centered at the origin of the spatial frequency domain, is depicted in Fig. 2(b). A deficiency in this spectrum is found in the different amplitudes of the two weak doughnut shaped light spots along the horizontal central axis. This deficiency is clearly noted comparing the amplitude profiles (along the horizontal axis) of the weak spots in Figs. 1(c) and 2(b). These profiles are respectively shown in Fig. 3(a) and Fig. 3(b). The amplitude asymmetry of the weak spots in Fig. 2(b) is originated in high order spectra terms, due to the pixelated hologram structure, that introduce noise contributions to the central region of the SPH spectrum field. A solution of this deficiency, in this particular case, is found by adopting new SPH carrier frequencies $u_0=v_0=\Delta u/4+\Delta u/32$, which avoids the perfect coincidence of the more significant high order contributions at the positions of the field spectrum spots. The SPH beam spectra spots obtained with these modified carrier frequencies, depicted in Fig. 2(c), presents an improved amplitude balance of the weak light spots. This improvement is evidenced in Fig. 3(c) that shows the amplitude profile of the weak spots of the spectrum in Fig. 2(c).

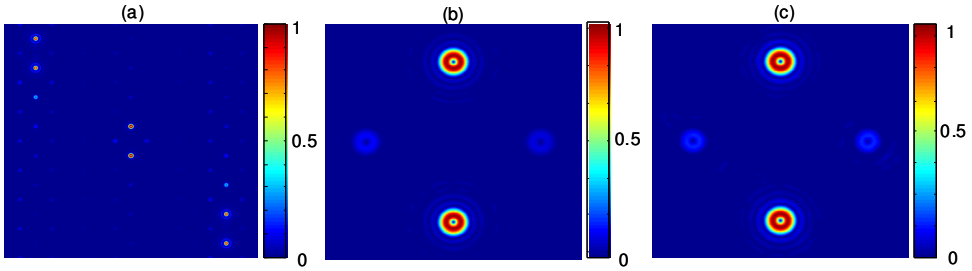

Fig. 2. Fourier spectrum modulus of the SPH that encodes the field $s_1(x,y)$: (a) central section and several high orders of the spectrum, (b) close view of the central spectrum region, and (c) central spectrum region for a modified SPH, with new carrier frequencies $u_0=v_0=\Delta u/4+\Delta u/32$.

#105592 - $15.00 USD Received 19 Dec 2008; revised 29 Jan 2009; accepted 6 Feb 2009; published 10 Feb 2009

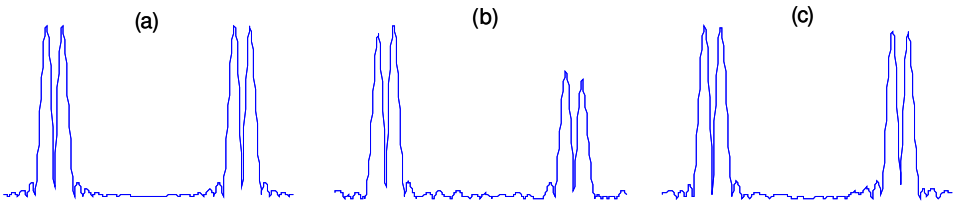

Fig. 3. Amplitude profiles along the horizontal axis of the weak spots in the Fourier spectra corresponding to (a) the encoded field $s_1(x,y)$, (b) the SPH with carrier frequencies $u_0=v_0=\Delta u/4$, and (c) the SPH with carrier frequencies $u_0=v_0=\Delta u/4+\Delta u/32$.

As second example we consider the complex field

$$s_2(x,y) = c\ \ [J_1(2\pi\rho_0 r)\cos(2\pi\xi_0 y+\theta)+b\cos(2\pi\eta_0 x)]. \tag{8}$$

This field is formed, on the one hand, by two first-order non-diffracting beams, with topological charges of opposite signs, propagating in the y-z plane, and two attenuated plane waves that propagate in the plane x-z. The attenuating factor for these waves is again b=1/10. Other different parameters for this encoded field is a support of radius R=438δx and beams carrier frequencies $\xi_0=\eta_0=\Delta u/48$. We assume again that the first root of the function $J_1[2\pi\rho_0 r]$ appears at the support edge and that the hologram frequency carriers are given as $u_0=v_0=\Delta u/4+\Delta u/32$, which correspond to the optimized values in the previous example. In this case we will assume that both the encoded field $s_2(x,y)$ and its SPH are additionally modulated by a Gaussian factor of radius $w=0.6\ R$. The purpose of this factor is to enable a fair comparison of the numerical results with the experimental implementation of the SPH, to be performed in section 4. In Figs. 4(a) and 4(b) we show the modules of the complex field $s_2(x,y)$ and its Fourier spectrum. The SPH that encodes the complex field $s_2(x,y)$, computed with Eq. (6), presents a Fourier spectrum modulus, whose central region, depicted in Fig. 4(c), is indistinguishable from the Fourier spectrum of the encoded field $s_2(x,y)$. This is an indication of the high SPH performance.

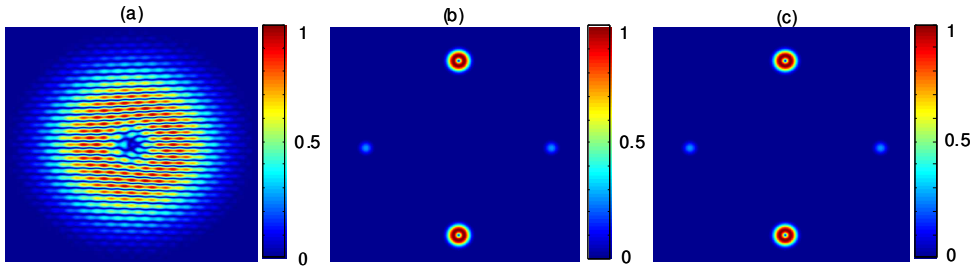

Fig. 4. Modulus of (a) the complex field $s_2(x,y)$, (b) modulus of its Fourier spectrum, and (c) Fourier spectrum modulus of the SPH that encodes the field $s_2(x,y)$.

Another complex field that we encode with a SPH is

$$s_3(x,y) = c\ \ [J_0(2\pi\rho_0 r)\cos(2\pi\xi_0 y)+b\cos(2\pi\eta_0 x)]. \tag{9}$$

Most of the comments specifying the field $s_2(x,y)$ and its SPH are also valid to specify the complex field $s_3(x,y)$ and its hologram. The main difference is that the first-order non-diffracting beam is replaced by a zero-order Bessel beam. In addition, the spatial frequency ρ_0 is determined in order that the edge of the field support coincides with the 5-th root of the function $J_0[2\pi\rho_0 r]$. It is also assumed in the present case that the encoded field and its SPH are modulated by the Gaussian factor already employed in the previous simulation. Figure 5 shows the modules of the complex field $s_3(x,y)$, and its Fourier spectrum, together with the modulus of the SPH Fourier spectrum. Again, the central region of the SPH spectrum

#105592 - $15.00 USD Received 19 Dec 2008; revised 29 Jan 2009; accepted 6 Feb 2009; published 10 Feb 2009

corresponds quite well with the spectrum of the encoded field, indicating a high SPH performance. This high quality SPH reconstruction has been enhanced again by the use of corrected SPH carrier frequencies $u_0=v_0=\Delta u/4+\Delta u/32$, instead of the originally proposed frequencies $u_0=v_0=\Delta u/4$. A general and detailed study of this carrier frequency optimization, for the discussed SPH, is out of the scope of the present study.

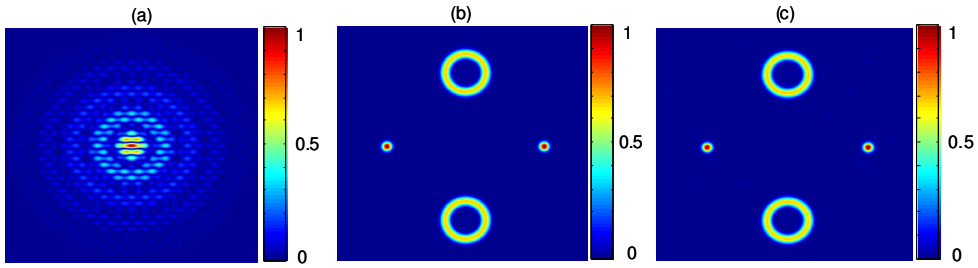

Fig. 5. (a). Modules of the complex field $s_3(x,y)$, and (b) of its Fourier spectrum. (c) Fourier spectrum modulus of the SPH that encodes the field $s_3(x,y)$.

In order to generate the complex fields defined in Eqs. (8) and (9) we perform an appropriate spatial filtering of the Fourier spectra of the corresponding SPHs. This filtering allows the transmission of the spectrum substructures that correspond to the beams composing each one of the encoded complex fields, and blocks the light spots that corresponds to the high order hologram terms. The encoded complex fields are obtained by performing the Fourier transform of the field transmitted by the spatial filter. The complete optical setup is depicted in Fig. 6 of section 4. At the output plane of this setup, all the beams that compose each one of the encoded complex fields appear within a common pupil, forming the interference patterns depicted in Figs. 4(a) and 5(a). The interfering beams in each case can be employed to interact in a nonlinear fashion e. g. within a photorefractive crystal [14]. However, this task is not studied here.

An alternative and useful application of the SPH discussed in Section 2 is the generation of multiple spots for optical manipulation. In this case the required output, formed by an array of compact spots, is usually obtained at the Fourier plane of the SPH displayed in the SLM.

4. Experimental implementation of SPHs for generation of multiple beams

The available modulator for encoding the SPHs is the SLM 1080P of Holoeye Photonics AG. This device is a reflective pixelated phase SLM with 1080×1920 pixels and a pitch $\delta x=8\mu m$, which provides modulation of 2π radians for laser light in the visible spectrum range. We employed this SLM to implement the SPHs of the fields defined in Eqs. (8) and (9), using a double Fourier transform setup, depicted in Fig. 6. In this setup, the SLM is illuminated by a collimated Gaussian He Ne laser beam, generated by a beam expander (BE), with a waist diameter of approximately $0.6R$, where $R=438\delta x$ is the radius of the circular pupil that limits the fields, $s_2(x,y)$ and $s_3(x,y)$, to be encoded. We employ a quasi-normal SLM illumination instead of a normal one to avoid the necessity of a cube beam splitter, which reduces the light throughput of the system. The Fourier spectra of the SPHs that encode the fields $s_2(x,y)$ and $s_3(x,y)$ are obtained at the focal plane of the first transforming lens L_1, where a spatial filter (SF) formed by an opaque screen with 4 small holes is placed. The holes in the SF only transmit the spectra light spots of the beams encoded in the SPHs. The reconstructed complex fields are obtained at the focal plane of the second transforming lens (L_2). The Fourier spectrum intensities of these fields are recorded with a CCD at the setup output plane. Employing such digitized experimental intensities, we compute the modules of the experimentally generated fields $s_2(x,y)$ and $s_3(x,y)$, which are depicted in Fig. 7. The obtained results are quite similar to the ones obtained by means of simulations [Figs. 4(a) and 5(a) respectively]. A high reduction of the amplitude at the edges, and at the low intensity areas, of

#105592 - $15.00 USD Received 19 Dec 2008; revised 29 Jan 2009; accepted 6 Feb 2009; published 10 Feb 2009

the experimentally generated fields, is probably due to a poor response of the employed CCD to low intensity light levels. A slight asymmetry in the experimentally recorded fields is mainly due to an imperfect centering of the input Gaussian beam, respect to the SPHs. This asymmetry that in reality is not so significant is enhanced by the pseudo color representation of the amplitude fields.

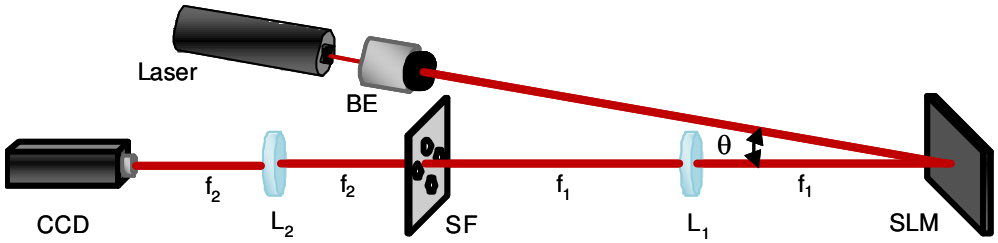

Fig. 6. Optical setup for experimental generation of multiple beams with a SPH.

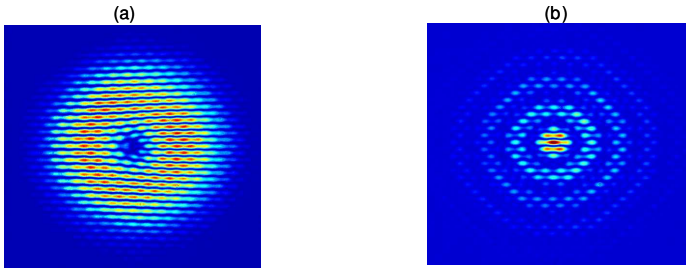

Fig. 7. Modules of experimentally generated complex fields (a) $s_2(x,y)$ and (b) $s_3(x,y)$.

5. Concluding remarks

The discussed SPH encodes an arbitrary complex field at the zero order of a sinusoidal phase carrier grating. This SPH exhibits important advantages: First, its encoding at the zero order of the carrier hologram allows an efficient use of the relatively reduced spatial frequency bandwidth of the pixelated SLMs, which are used to implement holograms. Second, the smoothness of the SPH sinusoidal carrier is convenient because electrically addressable SLMs do not display accurately high frequency modulation. Third, the power of the q-th order term, in the SPH Fourier series, presents a fast reduction, when the order q increases, because its amplitude is proportional to integer order Bessel functions $J_q(f(a))$, where $f(a)$ takes values between zero and the first root of $J_0(x)$. Although we developed the SPH for the simultaneous generation of multiple beams it also offers advantages for the generation of a single arbitrary complex beam. The demonstration of this fact was left out of the scope of the present report. Although theoretically the SPH can encode on-axis beams, in practice it is necessary to obtain the beams slightly off-axis. This phase shift is required to avoid the on-axis noise originated in the zero-order error modulation introduced by practical SLMs.

Acknowledgment

This study was financially supported by CONACyT, México, Project 24430.

#105592 - $15.00 USD Received 19 Dec 2008; revised 29 Jan 2009; accepted 6 Feb 2009; published 10 Feb 2009